AN INVESTIGATION ON THE PERFORMANCE OF AN IMIDAZOLINE BASED COMMERCIAL CORROSION INHIBITOR ON CO_2 CORROSION OF GAS-WELL TUBING STEEL BY EIS TECHNIQUE

A. Khavasfar[1], M. H. Moayed[2] and M. M. Attar[3]
mhmoayed@um.ac.ir

[1]Department of Materials Science & Metallurgicall Engineering, Shahid Bahonar University of Kerman
[2]Materials and Metallurgical Department, Faculty of Engineering, Ferdowsi University of Mashhad, Mashhad 91775-1111,
[3]Iran Polymer Engineering Department, Amirkabir University of Technology Tehran

Abstract: *The performance of an Imidazoline based commercial corrosion inhibitor in CO_2 corrosion of a gas-well tubing steel was studied by employing Electrochemical Impedance Spectroscopy (EIS) technique. Inhibitor performance was investigated by means of its efficiency at various concentration and also its behavior at various exposure time. EIS results showed that inhibitor interaction to the electrode surface obeys Lungmuir adsorption isotherm. Interpretation of some parameters such as R_{ct}, R_{pf}, C_{dl}, and C_{pf} associated to the equivalent circuit fitted to the experimental rsults showed that not only inhibitor efficiency and surface coverage improve by increasing in inhibitor concentration in the solution but also at constant inhibitor concentration both surface coverage and efficiency improve with exposure time and reach to their highest value after 4 hours.*

Keywords: *CO_2 corrosion, Inhibitor, EIS technique, Lungmuir adsorption Isotherm.*

1. INTRODUCTION

Carbon steels are still widely used in petroleum industry due to economical reasons. Usually these media contain high concentration of carbon dioxide and chloride ions. This environment causes sever corrosion of mild steel so; employing corrosion inhibitors is generally used to prevent corrosion. Organic corrosion inhibitors are the most effective means of protection to sever internal corrosion of carbon steel constructions in petroleum industry. Nitrogen-based organic surfactants such as imidazoline amids, imidazoline amido amines and their derivatives salts have been successfully used as inhibitors in this industry even without a clear understanding facts on the inhibition mechanism and performance of these inhibitors [1]. In order to investigate inhibitive performance and mechanism of these inhibitors various electrochemical techniques [2,3] in different condition from solution hydrodynamic conditions [4,5] have been investigated in detail. The performance of benzimidazole as a corrosion inhibitor in CO_2 environment was studied by D.A. Lopez and co-workers [6] employing Electrochemical Impedance Spectroscopy (EIS) and Linear Polarization Resistance (LPR) techniques. Carbon steel with two different microstructures (annealed and quenched-tempered \ Q&T) was used in deoxygenated 5% wt. NaCl solution which was saturated with CO_2 at 40°C. Their results showed that without inhibitor Q&T specimen showed a better corrosion resistance than annealed one. At the presence of corrosion inhibitor improved the corrosion resistance of annealed sample whereas for Q&T samples the opposite behavior was observed. They proposed that the protection mechanism of benzimidazole is based on reduction of protonated species at the cathodic sites (Fe_3C), leading to adsorption and blockage of these active areas and a relatively small delay in $FeCO_3$ precipitation. The morphology of cementite in each microstructures determines if such blockage is useful to reduce or activate the corrosion rate compared with the condition in which the inhibitor is absent. They concluded that the corrosion process and inhibitor efficiency is affected by heat treatment applied on steel. Imidazoline-base inhibitors are an active ingredient of inhibitor package for oil and

gas industry. They inhibit corrosion by blocking the area of metal surface by the adsorbed inhibitor film [7]. The imidiazoline molecule bonds the metal surface by the five-member ring structure containing two nitrogen atoms, which are loaded with electrical charges that make the ring hydrophilic, leaving the long hydrocarbon tail above the surface. The inhibition mechanism and adsorption/desorption of imidazoline amid on iron surface in saline solution saturated with 0.1 MPa CO_2 was investigated by X. Zhang and co-workers [8] employing EIS and potentiodynamic polarization techniques. The defined an adsorption potential in the potentiodynamic polarization curve of iron in test environment. When the potential is greater that adsorption potential, IM will be adsorbed from the electrode surface and results on increase in interface capacitance (C_{dl}) and decrease in transmission resistance ($R_{c.t}$). The increase of temperature and addition of chloride ions into solution decrease the adsorption potential of IM on iron surface. Inhibition mechanism of an imidazoline based inhibitor under multiphase flow condition using large diameter flow loop system was studied by Y. Chen and co-workers [9]. They employed EIS technique and from quantitative analyzing the Warburg parameter (b_f) they were able to determined conditions inhibitor film formation of steel surface. They found that the inhibitor film formation is correlated to exposure time and inhibitor concentration. The film becomes less porous with the increase in exposure time and concentration. The turbulent flow at the high rate of turbulence and bubble impact can degrade the inhibitor performance and increase the corrosion rate. Inhibitive performance of an imidazoline base corrosion inhibitor under multiphase flow was studied by Y. Chen et al [7] employing EIS technique. They demonstrated that EIS is an effective technique to investigate the inhibition performance of corrosion inhibitors in flow condition. Their experiment results revealed that the inhibitor film behavior is correlated to the exposure time and inhibitor concentration. This film becomes less porous with the increase in exposure time and concentration. The turbulent flow at the high rate of turbulence and bobble impact can degrade the inhibitor performance and increase the corrosion rate. They suggested EIS technique is a reliable method to evaluate corrosion inhibitor performance in flow condition. In this investigation electrochemical impedance spectroscopy (EIS) was employed to investigate the inhibitive performance and film characterization of an Imidazoline based commercial corrosion inhibitor formed on gas-well tubing steel in simulated gas well water saturated with carbon dioxide at various concentration and exposure time. The morphological characterization of used material was evaluated by scanning electron microscopy (SEM).

2. EXPERIMENTAL PROCEDURE

2.1. Specimen Preparation

The working electrode was selected form gas well tubing steel (composition given in Table 1 with a surface area of ~1.5 cm^2 for all measurements. Each specimen was soldered to copper wire for electrical connection. The copper wire was covered with a PVC tube to provide insulation from the test environment. Specimens were mounted in resin, and allowed to set overnight in air. All specimens were mechanically wet polished to a 600 grit SiC paper, then degreased with acetone prior to drying with air. Those specimens that were used in morphological investigation by scanning electrode microscopy (SEM) were mechanically polished up to 3µm and then etched by Pickral.

Table 1. Chemical composition of carbon steel (wt %).

C	Si	S	P	Mn	Ni	Cr	Fe
0.19	0.27	0.010	0.013	1.10	0.10	0.43	balance

2.2. Test solution

The salt water solution contains 96.2 gr/lit NaCl, 3.3 gr/lit $CaCl_2$ and 1.8 gr/lit $MgCl_2$ a mixture that is proposed by NACE 1D-182 simulating gas well solution [10].Test solution was deoxygenated with Ar gas for 3 hours to remove the dissolved O_2 in the solution and then was saturated with CO_2 gas for 3 hours. To make sure that the solution was saturated with CO_2, the pH of solution was measured prior to each test run. A pH value of 3.8 is acceptable [3,8]. The test solution was kept under a CO_2 atmosphere during testing. An Imidazoline based commercial inhibitor was used in this work. The effect of temperature on the inhibition efficiency of the inhibitor was investigated at 60°C using water

bath. All experiments were conducted in 1000 ml beaker. In general, 500 ml of test solution were used for each test. A commercial saturated calomel electrode (SCE) was used as a reference electrode for all experiments. The auxiliary electrode was a bright platinum 1mm diameter wire, area 2 cm^2 (Fig. 1).

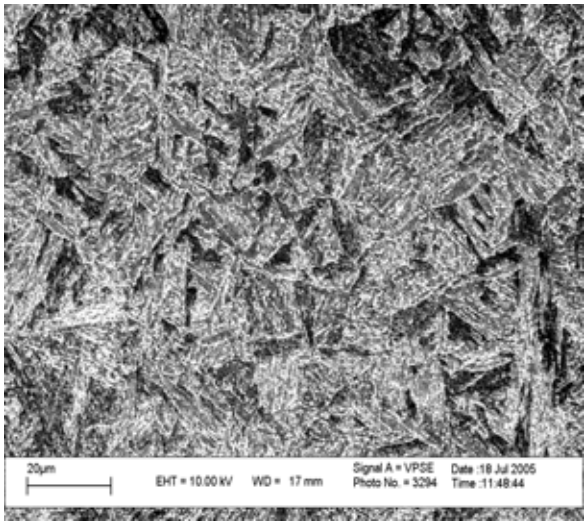

Fig. 1. SEM illustration of mild steel used in this work after etching in pickral.

2.3. Electrochemical Procedures

The EIS spectra were generated by an ACM workstation (ACM Instruments Co.) and then were analyzed using Auto-lab frequency responses analyzer software. The EIS measurements were carried out at rest potential with an amplitude of 10 to 20 mV AC potential in the frequency range of 30KHz to 0.1Hz. Prior to each experiment run, the corrosion potential of working electrode was allowed to be settled. During short term measurement of inhibitor performance EIS measurements was measured every hour for 8 hours. During this measurement electrochemical cell was under controlled CO_2 environment.

3. RESULTS AND DISCUSSION

Chemical composition of the tubing materials reveals that it is a very low alloy steel containing very low detriment elements in corrosion point of view (S and P) and also beneficial element such as Cr and Ni (table 1).

Morphological investigation of the specimen after etching in Nital shows that the alloy has been undergone initial heat treatment and then tempering. Almost detached and round carbide particles dispersed in needle-like ferittic matrix is the evident of such a heat treatment (Fig. 1). The backscattered image of SEM obtained from the investigated alloy also revealed such a morphological feature (Fig. 2).

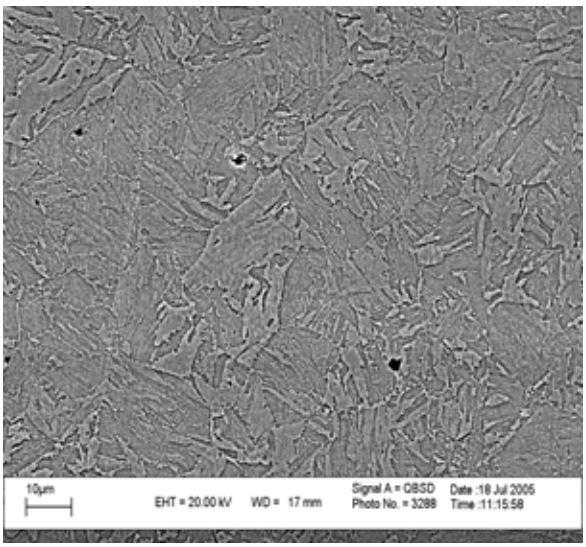

Fig. 2. Backscattered SEM image of mild steel used in this work after etching in pickral.

Adsorption isotherms are very important in understanding the mechanisms of organo electrochemical reactions. In order to obtain the Lungmuir adsorption isotherm the fractional coverage values (θ) as a function of inhibitor concentration (c) must be obtained. The apparent corrosion rate on inhibited steel is proportional to the ratio of surface converge (θ) and that not covered surface (1-θ) by the inhibitor. Surface coverage values have been evaluated in different concentration of inhibitor under the study of corrosion rate in an uninhibited and inhibited solution by means of the following equation:

θ was calculated from the R_{ct} measurements obtained from EIS results and then the following equation was implemented:

$$\theta = 1 - \frac{R_{ct(un-inhibited)}}{R_{ct(inhibited)}} \quad (1)$$

Where $R_{ct(uninhibited)}$ and $R_{ct(inhibited)}$ are the charge transfer resistance of working electrode at the absence and presence of inhibitor respectively. The Langmuir adsorption isotherm may be expressed as [11]:

$$\theta = \frac{Kc}{Kc+1} \quad (2)$$

Where K is the equilibrium constant for the adsorption process, c is the concentration of

inhibitor and θ is surface coverage:

$$\frac{c}{\theta} = \frac{1}{K} + c \qquad (3)$$

Fig. 3 illustrates the plot of c/θ versus inhibitor concentration (c) using EIS measurement method. Straight line with slope close to unity, indicating that adsorption of investigated commercial inhibitor on steel/saturated CO_2 solution obeys Lungmuir adsorption isotherm.

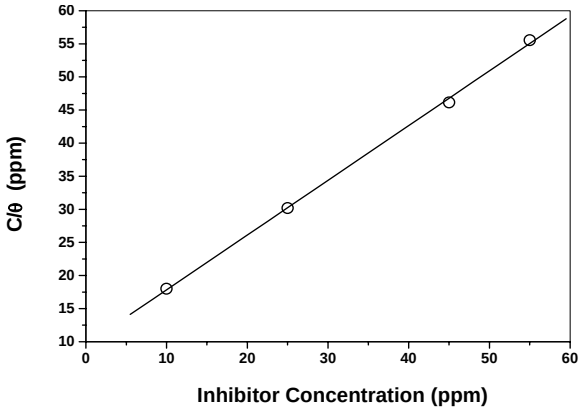

Fig. 3. Lungmuir isotherm curve fitting of corrosion data in CO_2 environment at the presence of inhibitor.

3.1. The effect of Inhibitor concentration

A typical Nyquist and Bode plots are illustrated for working electrode in blank CO_2 solution. The experimental result are almost fitted by simulated results obtained by Autolab analyzer software. Fig. 4 illustrates Nyquist and Bode plots for CO_2 corrosion of investigated steel in blank solution. Fig. 5/a illustrates the Nyquist plot of working electrode at the absence and presence of various concentration of corrosion inhibitor. It is evident that at a result of increasing inhibitor concentration the diameter of semicircle of Nyquist plot increases. This is attributed to the increased coverage of adsorbed inhibitor and the continuous strengthening and its protective ability as a result of increasing inhibitor concentration. The corresponding Bode plots (Fig. 5/b) shows at the presence of corrosion inhibitor two peaks appears at different frequencies. According the other investigations [7], the peak appeared at higher frequency is related to the film surface and at these frequencies the corrosion mechanism is controlled by the presence of surface film. Formation of one peak in the Bode plots (Fig. 5/b) at the absence of corrosion inhibitor shows the corrosion mechanism obeys Randles Model (Fig. 6/a).

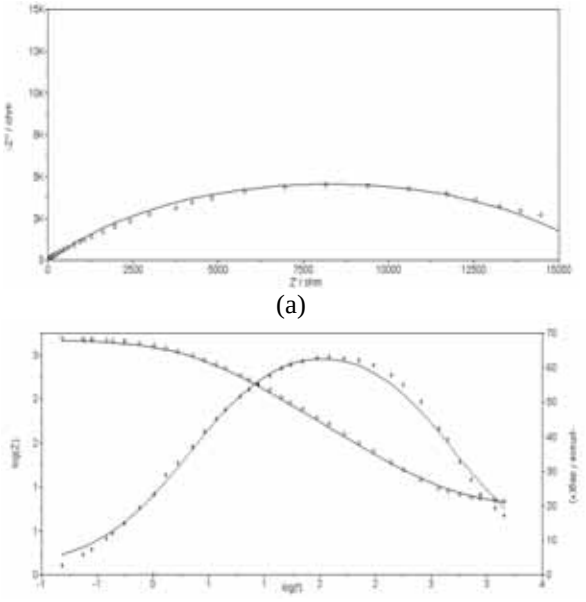

(a)

(b)

Fig. 4. EIS Nyquist (a) and Bode (b) plots for blank CO_2 solution. Experimental data with (marker) and fitting model with (solid line) are shown.

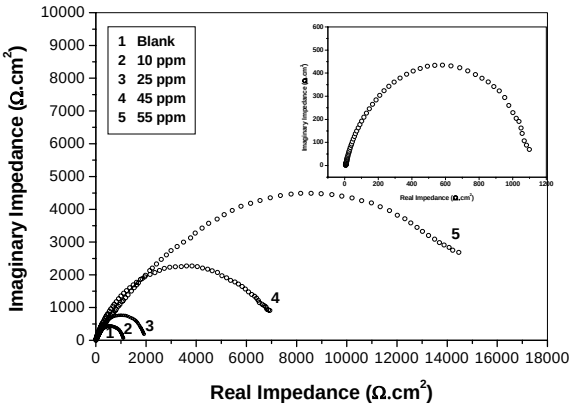

(a)

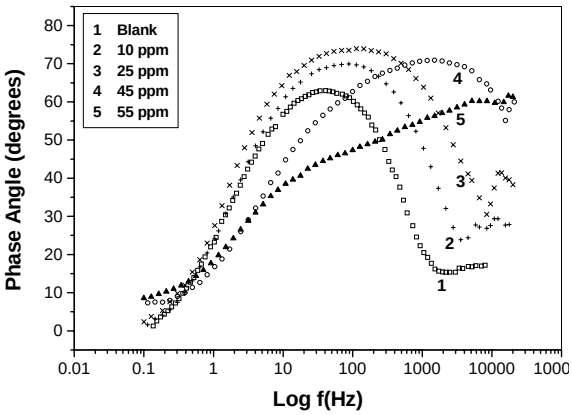

(b)

Fig. 5. a) EIS and Bode plots at different concentrations of corrosion inhibitor. In part (a) the Nyquist plot of working electrode in blank solution is highlighted.

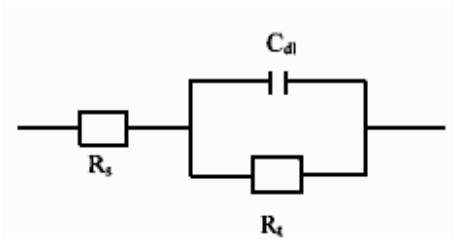

(a)

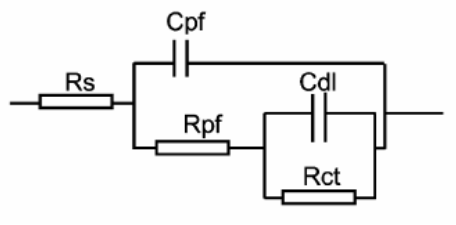

(b)

Fig. 6. Equivalent circuit used to represent the impedance results a) at the absence of corrosion inhibitor b) at the presence of corrosion inhibitor.

This is attributed to the lack of thermodynamic conditions for the formation of $FeCO_3$ film. The tendency for the formation of phase constant at high frequencies is appeared when the solution contains 25ppm corrosion inhibitor. Since this time constant is not properly distinguishable it can be claimed that at this concentration the film thickness and its coverage is negligible. At 45 ppm and particularly at 55ppm the formation of high frequency phase time constant is quiet pronounced.

The equivalent circuit proposed for mentioned system is similar to equivalent circuit that is usually proposed for coated metal surface and is illustrated in Fig. 6/b. In proposed equivalent circuit, (R_s) is the solution resistance, (R_{ct}) electrochemical charge transfer resistance, (C_{dl}) double layer capacitance, (C_{pf}) inhibitor film capacitance and (R_{pf}) the resistance of inhibitor film in pore areas. These parameters were calculated by fitting the EIS data into the circuit model and the results are shown in Table 2. As it can be seen, that the R_{ct} of the specimen at the presence of corrosion inhibitor is greater than the naked one, which suggests the formation of surface film on the electrode surface in the solution. As the inhibitor concentration in solution increases the R_{ct} increases gradually and steadily. The increase in R_{ct} indicates that the corrosion reaction of steel in CO_2 environment is inhibited by the development of surface film on the electrode. At the same time an increase on R_{pf} is also pronounced by increasing of inhibitor concentration. Fig. 7 illustrates the overall impedance that is associated to both R_{ct} and R_{pf} for different frequencies. It is apparent that for each frequency the amount of impedance increases by increasing inhibitor concentration in the test solution.

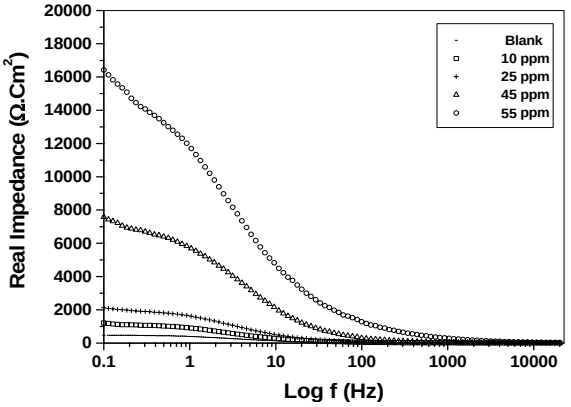

Fig. 7. Plots of real impedance vrs. log(f) for different concentrations of corrosion inhibitor.

Table 2. Evolution of fitted parameters for different inhibitor concentration.

C (ppm)	C_{dl} (μF)	$R_{c.t}$ (ohm.cm^2)	C_{pf} (μF)	R_{pf} (ohm.cm^2)	η%	θ %
Blank	55	460.0	-	-	-	-
10.0	25	1100.0	50	66.5	58.0	55.5
25.0	9.2	1960.0	33	102.0	76.5	83.0
45.0	0.13	7500.0	5.6	165.0	94.0	97.7
55.0	0.014	16300.0	0.24	645.0	98.0	99.8

On the other hand as a result of increasing of inhibitor concentration in the test solution, a gradual decrease in C_{dl} is observed. The value of C_{dl} is defined by the following equation:

$$C_{dl} = \frac{\varepsilon_{\circ}\varepsilon_{r}A}{d} \qquad (4)$$

where $\varepsilon_{\circ}$ is dielectric constant in vacuum, ε_r double layer dielectric constant, (A) the reaction surface area and (d) the distance between the plates of double layer capacitor. Since, in the investigated system all parameters except (A) are constant, any change in C_{dl} is directly related to change on (A). It is evident that gradual adsorption and polymerization of corrosion inhibitor on electrode surface area as a result of increase in inhibitor concentration may be the main reason for decrease in (A) and therefore in C_{dl}. The efficiency of inhibitor (η) was calculated by:

$$\eta\% = [1 - \frac{R_{c.t,b}}{R_{c.t,i}}] \times 100 \qquad (5)$$

where, $R_{ct,b}$ is the charge transfer resistance in the test solution without inhibitor and $R_{ct,i}$ is the charge transfer resistance in the test with inhibitor. Similar trend is proposed for calculation surface film coverage when inhibitor used in the system [12]. The following equation was used:

$$\theta\% = [1 - \frac{C_{dl,i}}{C_{dl,b}}] \times 100 \quad (6)$$

where, $C_{dl,b}$ is double layer capacitance in the test solution without inhibitor and $C_{dl,i}$ is double layer capacitance in the test with inhibitor. A similar trend in variation of inhibitor efficiency and its coverage is illustrated in Fig. 8. Since both items are directly related to inhibitor interaction with the metal surface by mean of chemi-sorption. This phenomena is almost the most possible interaction of an organic inhibitor in acidic environment.

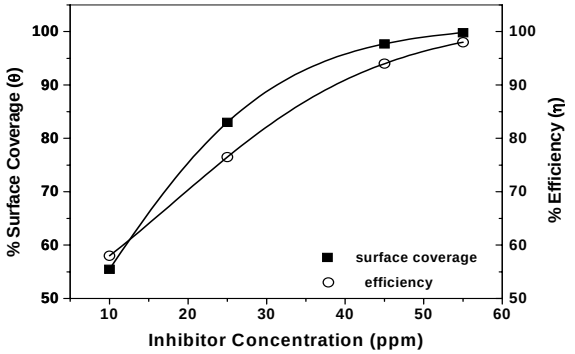

Fig. 8. Plots of inhibitor coverage and its efficiency as a function of inhibitor concentration.

3.2. Time dependence Inhibitor performance

The Nyquist diagram for working electrode obtained after 0.5, 2, 4, 6 and h hours of immersion at 40ppm inhibitor concentration in CO_2 environment is illustrated in Fig. 9. The magnitude of total impedance increases continuously with time. All experimental plots have a depresses semicircle shape in complex plane. The efficiency calculated by Eq. (5) at various time revealed that the inhibitor efficiency reaches to limit of 97% after 4 hours immersion. Implementing similar equivalent circuit as Fig. 5 and calculating the variation of parameters of the circuit revealed an increase in R_{ct} and R_{pf} with exposure time (Table 3). The value of R_{pf} can be calculated by the following equation:

$$R_{pf} = \frac{d}{K_p . A . \xi^{2.5}} \quad (7)$$

Table 3. Evolution of fitted parameters for 40ppm inhibitor concentration at various exposure time.

Exposure time (Hour)	C_{dl} (μF)	$R_{c.t}$ (ohm.cm^2)	C_{pf} (μF)	R_{pf} (ohm.cm^2)	η%	θ %
Blank	55	460.0	-	-	-	-
0.5	0.33	6200	8.1	148	93.00	92.58
2.0	0.14	12600	0.85	259	96.40	96.34
4.0	0.13	14100	0.67	465	96.75	96.73
6.0	0.12	14300	0.52	492	96.80	96.78
8.0	0.11	14600	0.46	566	96.85	96.84

where d is the thickness of adsorbed inhibitor, Kp is the electrolyte conductivity the inhibitor film porosity, A electrode surface area and ξ is the mean value of inhibitor film porosity. ξ is also defined by the following equation:

$$\xi = \frac{A_p}{A} \quad (8)$$

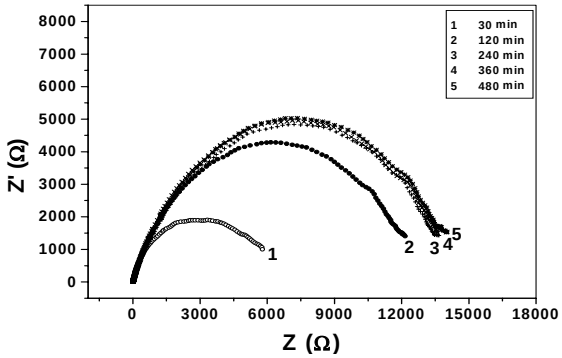

Fig. 9. EIS Nyquist plots for 40ppm inhibitor concentration at different exposure time.

where A_p is the total surface area associated to the porosity from the electrode surface area. An increase to the value of R_{pf} with exposure time is directly associated to values of (d) and (ξ) in equation (7). Inhibitor adsorption on the electrode surface and then inhibitor molecules polymerization on the electrode surface area leads to an increase to its thickness and also a decrease on mean value of inhibitor porosity. This is illustrates schematically in Fig. 10. It is shown that an inhibitive characteristic such as adsorption, polymerization, coverage and thickness, of inhibitor is improved by time.

The capacitative behavior of film inhibitor is defined by C_{pf} which is related to the other parameters by the following equation:

$$C_{pf} = \frac{\varepsilon_\circ \varepsilon_f A}{d_f} \quad (9)$$

where (ε_f) is dielectric constant associated to inhibitor film and (d_f) is plate distance of inhibitor film capacitor.

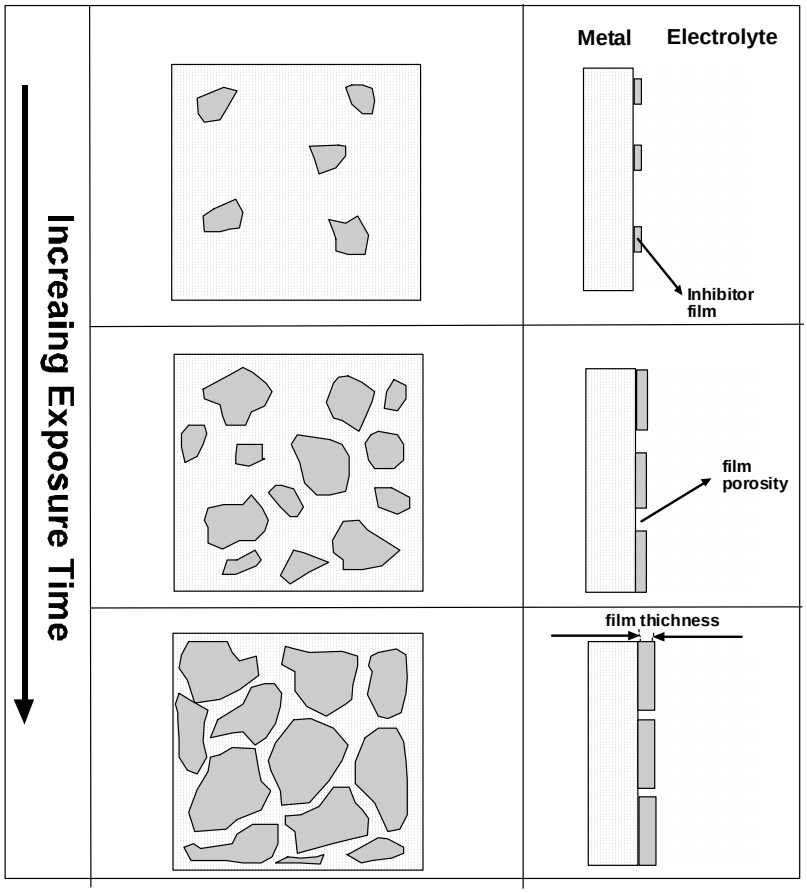

Fig. 10. Schematic illustration of inhibitor adsorption, polymerization and thickening on the electrode surface. The inhibitor is indicated by gray colonies.

It is clear that decreasing of C_{pf} is directly related to an increase in (d_f) due to increase in inhibitor film thickness. On the other hand a decrease in C_{pf} can also be related to the decreasing in (ε_f). As exposure time increases, the amount of inhibitor porosity decreases and the specimen surface is covered by a continues and more compact inhibitor film. This causes on decrease in (ε_f) and therefore C_{pf}. Table 4 shows dielectric constant for some media. It is evident that dielectric constant for organic coatings depending on their properties is 0.1 to 0.05 of water dielectric constant.

Table 4. A comparison on dielectric constant for different media.

Material	ε
vacuum	1
water	80.1 (20° C)
organic coating	4 - 8

The similarity of degree of coverage by inhibitor and also inhibitor efficiency which were both calculated by applying equations 5 and 6 to exposure time is illustrated in Fig. 11. The inhibitor film covers over 96% of the specimen surface just after 4 hours contact with the specimen surface area. The value of coverage becomes independent of exposure time after 4 hours. This means that after this period all the inhibitor concentration in the test solution is participated to the surface coverage.

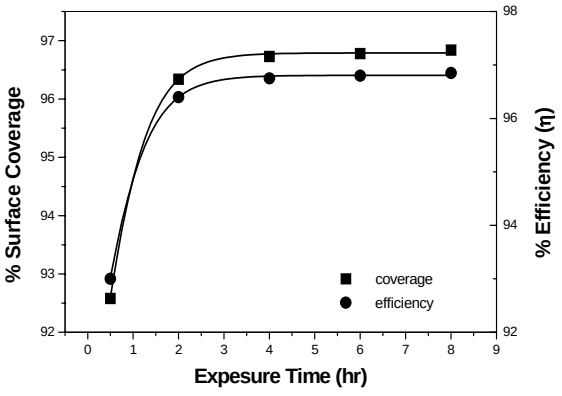

Fig. 11. Plots of inhibitor coverage and efficiency evolution for 40ppm inhibitor concentration.

4. CONCLUSION

The main conclusions drawn from this study are:

1. Electrochemical impedance spectroscopy (EIS) has been shown to be a useful tool for studying corrosion process in the presence of CO_2 and evaluation of the adsorption mechanism of a commercial corrosion inhibitor.
2. Inhibitor efficiency and coverage are improved as the inhibitor concentration increases in the CO_2 solution. Highest degree of coverage and efficacy were obtained at 55ppm inhibitor concentration.
3. The fitting results showed that the degree of inhibitor efficiency and coverage is time dependence. After 4 hours immersion of working electrode in solution containing 40ppm inhibitor the degree of inhibitor coverage and efficiency reach to their limit.

REFERENCES

1. T. Hong, W. P. Jepson, "Corrosion Iinhibitor Studies in Large Flow Loop at High Temperature and High Pressure", Corrosion Science, vol. 43, pp. 1839-1849, (2001).
2. A. Lopez, S .N. Simison, S. R. De Sanchez, "The Influence of Steel Microstructure on CO_2 Corrosion. EIS Studies on the Inhibition Efficiency of Benzimidazole", Electro-chemical Acta, vol. 48, pp. 845-854, (2003).
3. L. Mora-Mendoza, S. Turgoose, "Fe_3C Influence on the Corrosion Rate of Mild Steel in Aqueous CO_2 Systems Under Turbulent Flow Conditions", Corrosion Science, vol. 44, pp. 1223-1246, (2002).
4. T. Hong, Y. H. Sun, W. P. Jepson, "Study on Corrosion Inhibitor in Large Pipelines under Multiphase Flow using EIS", Corrosion Science, vol. 44, pp. 101-112, (2002).
5. D. A. Lopez, S. N. Simison, S. R. de Sanchez, "Inhibitors Performance in CO_2 Corrosion EIS Studies on the Interaction Between their Molecular Structure and Steel Microstructure", Corrosion Science, vol. 47, pp. 735-775, (2005).
6. D. A. Lopez, T. Perez, S. N. Simison, "The Influence of Microstructure and Chemical Composition of Carbon and Low Alloy Steels in CO_2 Corrosion. A State-of-the-Art Appraisal", Materials and Design, vol. 24, pp. 561–575, (2003).
7. Y. Chen, W. P. Jepson, "EIS Measurement for Corrosion Monitoring under Multiphase Flow Conditions", Electrochimica Acta, vol. 44, pp. 4453-4464, (1999).
8. X. Zhang, F. Wang, Y. He, Y. Du, "Study of the Inhibition Mechanism of Imidazoline Amide on CO_2 Corrosion of Armco Iron", Corrosion Science, vol. 43, pp. 417-431, (2001).
9. Y. Chen, T. Hong, M. Gopal, W. P. Jepson, "EIS Studies of a Corrosion Inhibitor Behavior Under Multiphase Flow Conditions", Corrosion Science, vol. 42, pp. 979-990, (2000).
10. NACE International Publication, 1D182 (2005).
11. K. Naicker, "Surface Chemistry", University of Cape Town, pp. 10-15, (2005).
12. C. C. Nathan, "Corrosion Inhibitors", Betz Laboratories Inc, NACE, pp. 61-88, (1973).